Characterization of candle soot obtained from combustion of candle wax for the removal of methylene blue

Nandini Choudhary* and Armila Nyachhyon (Rajbhandari)*

* Central Department of Chemistry, Tribhuvan University, Kirtipur, Kathmandu, Nepal.

Abstract: Carbonaceous candle soot (CS) was prepared from combustion of candle wax in the laboratory. Thus prepared material has been characterized by energy dispersive X-ray analysis (EDX), X-ray diffraction (XRD), fourier transform infrared spectroscopy (FTIR), scanning electron microscopy (SEM). Surface area, methylene blue number (MBN), and iodine number (IN) were also investigated. EDX clearly showed high carbon content. XRD exhibited well defined graphitic domain structure. Oxygen functionality has been observed on the surface by FTIR. The specific surface area of CS, was found to be 242.46 m^2/g. Thus prepared CS was used for the removal of dye from aqueous solution by batch adsorption studies. Methylene Blue (MB) was used as a model dye. The adsorption parameters such as contact time, initial concentration of MB and adsorbent dosage, and pH were also examined. The optimum pH was found to be 10 while optimum time and adsorbent dose was found to be 2 hrs and 0.25 g/L respectively. After optimizing parameters, CS as an adsorbent have been used to remove MB where a significant 97% MB adsorption was observed. To evaluate adsorption behaviors of CS, different adsorption isotherm models have been tested. Langmuir isotherm and Temkin isotherm model revealed the chemisorption type of adsorption perceived in CS. The maximum monolayer coverage (Q_m) was found to be 17.95 mg/L with the dimensionless separation factor $R_L < 1$ indicating a favorable sorption condition. Therefore, it might be an impressive alternative for the treatment of colored wastewater discharged from many industrial outlets including textile.

Keywords: Candle soot; Methylene blue dye; Langmuir adsorption isotherm.

Introduction

Carbon is a versatile material having different forms. Diamond, activated carbon, and graphite are well-known allotropic forms that have demonstrated its significance in a variety of disciplines. Furthermore, carbon nanotubes, nano crystals, nano spheres, fullerene, and graphene nanosheets have proved their utility in nano electronics, sensors, micro-electrical devices, drug delivery and adsorption of pollutants [1]. Each have its own exclusive properties and benefits, nevertheless, all these materials are synthesized using complicated processes of installation and are costly. In these days, environment friendly and cost-effective precursor materials such as coconut, peanut hull, rice husk, orange peel, fly ash, bamboo waste, and biomass have been investigated [2] to obtain low cost activated carbon which is then used as an adsorbent [3, 4] to remove dye pollutants from water.

Recently, soot, a form of nano carbon, has demonstrated good adsorption competency. These soot particles are generated from lampblack and candle wax flames as well. Candles have been used as a source of light since prehistoric eras and in various indoor environments [5]. Candles are generally is made up of paraffin having crystalline mixtures of hydrocarbons comprising of linear n-alkane and branched iso- and cyclo-alkanes with carbon

***Author for correspondence*:** Armila Nyachhyon (Rajbhandari), Central Department of Chemistry, Tribhuvan University, Kirtipur, Kathmandu, Nepal.
Email: armila.rajbhandari@cdc.tu.edu.np; https://orchid.org/0000-0003-4837-328X
Received: 26 Jan, 2026; Received in revised form: 24 Mar, 2026; Accepted: 30 Mar, 2026.
Doi: https://doi.org/10.3126/sw.v19i19.95640

chain lengths ranging from C_{16} – C_{30} [6,7,8] and are obtained from crude petroleum oil [9,10, 11,12]. Michael Faraday in 1860 [4, 6] described the mechanism of the combustion taking place in a candle flame as a diffusion flame with wax serving as fuel and the wick as transport mode of the fuel by capillary forces. Literatures [13, 14] revealed that the pyrolysis of paraffin and other waxes results in smaller hydrocarbons that resemble acetylene, followed by the creation of aromatic hydrocarbons, which is the method through which soot is formed. Polyaromatic hydrocarbons (PAHs) are made up of small individual aromatic molecules and alkyl groups. The candle soot's nuclei are created by the binding of many of these PAHs. Following surface reactions, the nuclei subsequently coagulate, leading to the development of soot particles and agglomeration. In accordance with the Figure 1, there are four main processes in the soot creation process: (i) homogenous nucleation from a semi-solid droplet of carbon particles, (ii) nuclei particle coagulation, (iii) surface reactions such as growth and oxidation, and (iv) particle agglomeration [13-14].

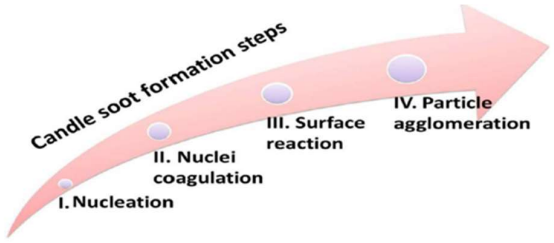

Figure 1: Four major steps of soot formation [15].

Several researchers have provided information on soot characteristics, soot volume fraction and soot morphology [15, 16, 17]. In this study, candle soot has been prepared, characterized and utilized to remove cationic dye from water. Here, methylene blue (MB) was used as model dye pollutant to study the adsorption behaviors of candle soot as MB is one of the most heavily consumed colorant in the dye business [18] and is frequently used to color silk, wool, cotton, and paper.

Materials and Methods

Candle wax used in this study was purchased from local market of Kathmandu, Nepal and used without further purification. Phosphoric acid, iodine, sodium thiosulphate, methylene blue and sodium hydroxide pellets were obtained from Merck life Science Pvt. Ltd., India.

All the solution has been prepared in distilled water.

Preparation of Candle soot (CS)

Candle wax was placed in a simple laboratory fume cupboard. The candle was lighted with a match and allowed to burn. A flat ceramic tile plate was placed above the flame of the candle to collect soot emitted from the candle flame. Initially, the height of plate and burnt candle is two inch. After some time, size of candle became small so height had been adjusted accordingly. When the amount of soot approximately equal to 10 g was collected, the experiment was terminated. Thus obtained soot was then stored in a glass container.

Characterization of Candle soot (CS)

The phase state of prepared candle soot was investigated using X-ray Diffractometer (D2 phaser , Bruker, Germany) set at an accelerating voltage of 40KV and current 40mA with Cu-Kα radiation (λ=1.54184 A°) in the diffraction angles ranging from 10 to 50 degrees. Fourier Transmission Infrared Spectroscopy (Schimatdzu, Model No IR Tracer-100 Japan) was used to study for the occurrence of a surface functional groups. The FTIR spectra of candle soot was recorded at 4000-400 cm^{-1} wave number. The surface morphology of as prepared candle soot was studied with scanning electron microscopy (SEM) (Hitachi S-4800) at an accelerating voltage of 10 KV. The elemental composition and chemical makeup of prepared candle soot was examined by the energy dispersive x-ray analysis (EDX) in conjugation with SEM (Gemini SEM 500, Zeiss).

Determination of meso porosity by Methylene Blue Number (MBN) Method

For the determination of the methylene blue number, 10 mg of the prepared candle soot (CS) was introduced into a 250 mg/L methylene blue solution. The suspension was vigorously mixed to achieve uniform dispersion and then placed on a shaker at 200 rpm for 180 minutes at room temperature to facilitate adsorption. Following this, the mixture was filtered, and the residual concentration of methylene blue was measured using a UV-Vis

spectrophotometer at 664 nm. The MB_N was calculated using equation 1:

$$MB_N = \frac{C_o - C_e}{M} \times V \ldots\ldots\ldots\ldots\ldots\ldots (1)$$

Where,

C_0 = Initial concentration (mg/L)

C_e = Equilibrium concentration (mg/L)

M = Weight taken (g)

V = Volume of solution (L)

Determination of micro porosity by Iodine Number (IN) Method

In a conical flask, 0.1 g of candle soot (CS) was placed, followed by the addition of 5 mL of 5% HCl, which was then heated to boiling and allowed to cool. Subsequently, 10 mL of 0.1 N iodine solution was introduced into the flask, and the mixture was vigorously shaken in a mechanical shaker for 15 minutes. Afterward, it was filtered and the filtrate was titrated with standard thiosulphate solution using starch as an indicator. This process was repeated three times consecutively. The quantity of thiosulphate consumed was measured, and the iodine number was then calculated using the equation 2

$$IN = \frac{\text{Amount of iodine adsorbed by carbon}}{\text{Mass of Activated carbon}} \ldots (2)$$

Determination of specific surface area [19]

For the determination of surface area of as prepared candle soot (CS), the methylene blue number (MBN) and iodine number (IN) were taken into consideration using equation (3)

$$S_{(m^2g^{-1})} = 2.28 \times 10^2 - 1.01 \times 10^{-1}MBN + 3 \times 10^{-1}IN + 1.05 \times 10^{-4}MBN^2 + 2 \times 10^{-4}IN^2 + 9.38 \times 10^{-4}\ MBN\ IN \ldots\ldots\ldots\ldots\ldots\ldots (3)$$

Batch Adsorption Studies

The adsorptive removal of MB from an aqueous solution using candle soot (CS) was carried out using batch adsorption method. MB solution in the concentration range (20-100 mg/L) were prepared from MB in distilled water. The required amount of CS was added into an Erlenmeyer flask containing MB solution. The flask was shaken in a mechanical shaker for 2 hrs. The concentration of residual MB after equilibrium was determined using a UV-Vis spectrophotometer. The percentage removal and the amount of MB adsorbed were calculated using following relations (4 and 5) [20].

$$qe = (Co - Ce)\ X\ V / m \ldots\ldots\ldots\ldots\ldots\ldots\ldots\ldots (4)$$

$$\%\ removal = (C_0 - Ce)\ /C_0\ X\ 100\% \ldots\ldots\ldots\ldots\ldots (5)$$

Results and Discussion

Characterization of Adsorbent

Energy Dispersive X-Ray Analysis (EDX)

To explore the elemental composition EDX of candle soot (CS) was carried out. Figure 2 is a typical energy dispersive x-ray spectrum of CS. The spectrum shows that CS contains more than 95% carbon and trace quantity of oxygen and silicon and are distributed homogeneously. In mapping image, three different colors were applied to simply describe the mapping image of carbon, oxygen and silicon. The presence of carbon was shown in red color whereas the other two elements like oxygen and silicon were represented by green and yellow color respectively.

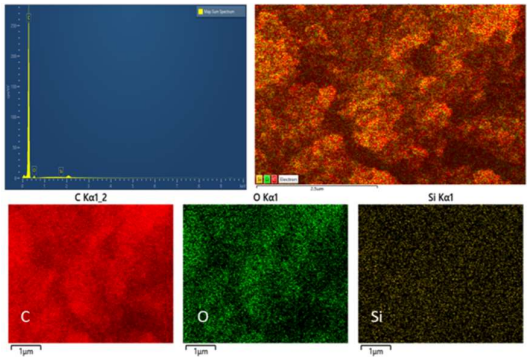

Figure 2: EDX pattern and elemental mapping image of candle soot: Carbon is represented by red colour, Oxygen is represented by green colour and Silicon is represented by yellow colour.

From the Table 1, one can clearly see the highest atomic value of carbon i.e. 97.20% while oxygen and silicon were found to be 2.78% and 0.02% respectively, indicating that as prepared adsorbent was found to be pure and has high content of carbon.

X-Ray Diffraction Analysis

To study the phase state, XRD has been recorded. Figure 3 displays the XRD pattern of as prepared candle soot (CS). The two prominent diffraction peaks at 24.6 $2\theta^{o}$ and 43

Table 1: Elemental distribution.

Elements	Atomic percentage
Carbon	97.20
Oxygen	2.78
Silicon	0.02

2θ° were observed in XRD pattern which corresponds to the (002) and (100) planes respectively. According to JCPDS card (No-41-1487), the XRD pattern is an indication of a characteristic hexagonal graphitic lattice structure. The intense peak at 24.6 *2θ°* matches to graphite

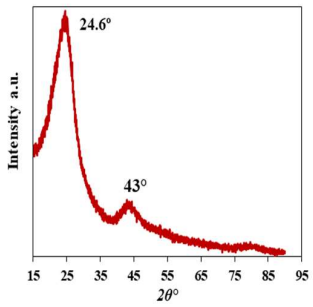

Figure 3: XRD pattern of candle soot.

(002), indicated the presence graphitic materials [15]. The peak at 43 *2θ°* caused by interlayer and intralayer scattering of graphene stacks indicated the presence of graphitic domain structure [15].

Fourier Transfer Infrared Spectroscopy Analysis

Figure 4 displays the FTIR spectra of prepared candle soot (CS). In spectra, there is a large band at 3330 cm^{-1} that is attributed to the -OH stretching vibration caused by the intermolecular hydrogen bonding of polymeric substances such as alcohols, phenols, and carboxylic acid. Similarly, the modest peak at roughly 2918 cm^{-1} in FTIR spectra

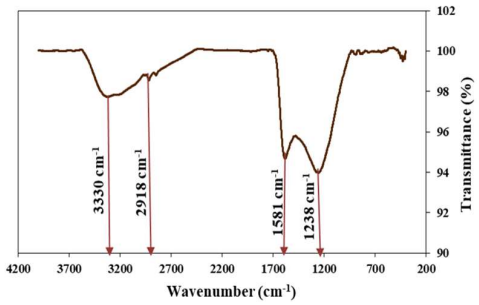

Figure 4: FTIR spectrum of candle soot.

demonstrates the symmetric vibration of CH_3 gathered from the inner flame. The soot from the inner flame zone has thick and intense CH_3 bands, indicating the presence of a high proportion of CH_3 (organic) as a result of incomplete combustion/oxidation of the candle [21]. The spectra at 1581 cm^{-1} indicates C=C aromatic vibration. The peak in the surrounding area, 1238 cm^{-1}, indicates vibrational C-O stretch [22] which is another evidence for oxygen surface functionality on candle soot. Figure (5 a,b,c) displays the SEM pictures of as prepared candle soot (CS) at 2, 2.5 and 5 µm magnification respectively. The surface morphology of the carbon deposit obtained was seen to be non-uniform. There are several grains of nanomaterial in the micrograph. The candle wax flame soot particles are extremely small with a majority of the particles about 0.2 µm in diameter. The irregular carbon particles are found to be joined together forming agglomerations of soot particles. The SEM image does not show any carbon nanotubes and the soot particles could not be classified as nanospheres.

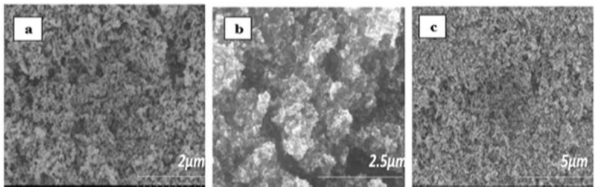

Figure 5: Scanning electron micrograph (SEM) of soot obtained from the combustion of candle wax.

Methyl Blue Number (MBN), Iodine Number (IN) and Specific Surface Area (SSA)

The MBN, IN and surface area of candle soot (CS) were obtained by using equation 1, 2, 3 respectively and results are presented in Table 2. MBN and IN represented that CS consists of meso and micro pores. The surface area was found to be 242.46 m^2/g.

Table 2: MBN, IN and SSA of candle soot (CS).

Sample name	MBN (mg/g)	IN (mg/g)	SSA (m^2/g)
CS	16.19	50.8	242.46

Adsorption studies

Adsorption parameters

To find the adsorption efficiency of candle soot (CS) different adsorption parameters have been scrutinized. Here, MB was used as a model dye. The results are presented in Figure 6. To evaluate the adsorption capacity, the CS was treated with a MB solution under different conditions (Figure 6). The dependency of MB adsorption on pH was shown in Figure 6a. The adsorption percentage was low at acidic pH, and it increased with increasing pH. Almost 97 % of MB was adsorbed at basic pH. In acidic pH, the cationic dye must compete with high concentrations of H^+ ions to form bonds with the surface-active sites. At basic pH 10, the CS was negatively charged and efficiently adsorbs the positively charged MB, thereby removing 97% of it. After pH 10, there may be the development of aqua complexes which causes the decrease in the percentage of adsorption, delaying dye sorption [23, 19]. The optimum amount of CS required to remove 50 mg/L of MB was studied by increasing the adsorbent dose from 0.20 g/L to 0.33 g/L (Figure 6b). At low doses, the removal percentage was less than 90 %. Further increasing the dose to 0.25 g/L, MB was removed by 97%, suggesting 0.25 g/L was the optimum dose required to remove 50 mg/L of MB (Figure 6b). The time required to attain equilibrium of MB adsorption, was analyzed by measuring the adsorption percentage at different times (Figure 6c). More than 80% was adsorbed within 10 minutes, and the adsorption rate increased with time, reaching equilibrium by adsorbing 97% of the MB within 2 hrs (Figure 6c). This suggests 2 hrs of contact time is required for the 97% adsorption of MB from aqueous solution. The adsorbing capacity of CS was then investigated by varying the concentration of MB (Figure 6d). CS can remove 97% up to 50 mg/L of MB. Increasing the initial concentration of MB, the adsorption percentage reduced nearly to 80% at 100 mg/L. Initially, the MB adsorption capacity was high because there was a large availability of adsorption sites. As the concentration increased, the active sites of the adsorbate became occupied, resulting in a decrease in the adsorption percentage.

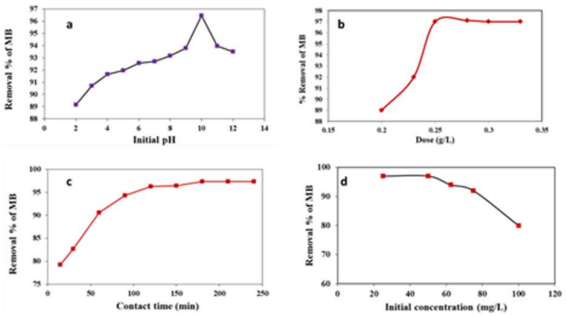

Figure 6: Effect of initial pH, adsorbent dose, contact time and initial concentration on removal of MB dye by using CS adsorbent.

Adsorption Isotherm Studies: To evaluate the feasibility, three different isotherm models have been tested.

a. Langmuir isotherm model

It is widely applied model to describe experimental adsorption data based on the assumption that maximum adsorption corresponding to saturated monolayer of adsorbate molecule on adsorbent surface with a constant energy and no further adsorption. The Langmuir adsorption equation can be represented as;

$Qe = Q_m bC_e / 1+bCe$ .....……(6)

The linear form of Langmuir expression is expressed as;

$1/Qe = 1/Q_m bC_e + 1/Q_m$ .....(7)

Where, Qe (mg/g) is the amount of adsorbate adsorbed per unit mass of adsorbent; Ce(mg/L) is the equilibrium concentration of the adsorbate in solution after adsorption; Qm (mg/g) is the maximum adsorption capacity corresponding to monolayer coverage of adsorbents and b (L/ mg) is the adsorption equilibrium constant. Langmuir adsorption isotherm is presented in Figure 7.

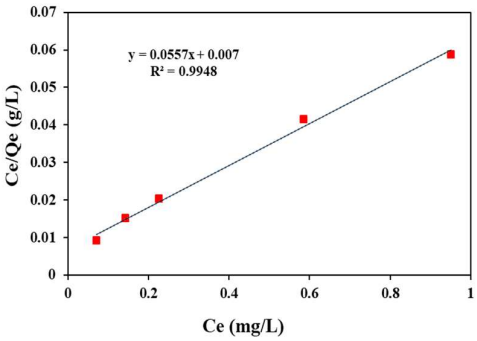

Figure 7: Langmuir adsorption Isotherm.

Here, the value of Qm and b are presented in Table 3 which was calculated from the slope and intercept of the Ce/Qe versus Ce plot. The sorption capacity of CS was found to be 17.95 mg/g found to be in good agreement with literature values [24]. The Langmuir isotherm constant (b) was found to be 7.96 L/mg which indicates free energy of adsorption. The essential feature of Langmuir adsorption isotherm can be expressed in terms of dimensionless constant called separation factor or Langmuir parameter (R_L) which was found to be 0.1. This R_L value lies between 0 and 1 indicating the favourability of adsorption. Here, R_L was calculated by equation (8);

$$R_L = 1/(1+ bC) \quad \text{.....(8)}$$

Where, C_i = Initial concentration (mg/L) and b = Langmuir constant. The correlation coefficient R^2 value is closer to unity which indicated that linear isotherm is fitted for CS sample.

b. Freundlich isotherm model

The adsorption data was also tested through Freundlich adsorption isotherm model. The model explains the non-ideal sorption that involves heterogeneous surface energy system and is expressed by equation (9).

$$Q_e = K_F (Ce)^{1/n} \quad \text{……(9)}$$

The linear form can be written as;

$$\log Q_e = \log K + \log Ce \quad \text{..……..(10)}$$

where, K_F and n (dimensionless constants) are the Freundlich adsorption isotherm constants, K_F indicates adsorption capacity which was found to be 16.31 mg/g for CS . The slope 1/n ranging between 0 and 1, is favorable adsorption condition and was found to be 0.54 (Table 3) which indicates the favorable adsorption behavior of MB from aqueous solution by CS sample however the correlation coefficient value obtained from Freundlich isotherm was found to be 0.9888 which appeared to be lower than the Langmuir isotherm value i.e. 0.9948. It clearly revealed that Langmuir model was best fitted one.

c. Tempkin isotherm model

After observing above two models, the effect of interaction of adsorbate and adsorbent was studied by Temkin adsorption isotherm model. This model assumes that heat of adsorption of all the molecules in the layer would decrease linearly rather than logarithmically with coverage due to adsorbate adsorbent interaction and adsorption is characterized by uniform distribution of binding energy up to some maximum binding energy. The linearized Temkin equation is given by the following equation (11 and 12).

$$Q_e = (RT/b) \log K_T C_e \quad \text{.....(11)}$$

$$Q_e = B\ln K_T + B\ln C_e \quad \text{.....(12)}$$

Where, (RT/b) = B, K_T = Tempkin isotherm equilibrium binding constant (L/g), which corresponds to maximum binding energy, b = Tempkin isotherm constant, R = Universal gas constant (8.314 J/ mol/K), T = temperature at 298K, B = constant related to heat of sorption (J/mol). The Tempkin constants RT and b is calculated from the slope and intercept of Q_e as a function of $\ln C_e$ and the results are presented in Table 3, where heat of sorption (B) was found to be 0.24 J/mol. The maximum binding energy (K_T) was found to be 3.21 L/g for CS indicates greater chemisorption type of interaction between adsorbate and adsorbent.

Comparative study of adsorption capacity candle soot with other literature value

The maximum adsorption capacity (Q_m) of CS for MB was compared with earlier investigations which are tabulated in Table 4 and was found to be in agreement with literature values [4, 25].

Conclusion

The study showed that soot produced from candle wax flame comprised of significant amount of amorphous carbon. EDS analysis also provided a strong evidence of significant amount of carbon in candle soot particles. The surface area of CS, was found to be 242.46 m^2/g having micro and meso pores. Results revealed that more than 97% of MB, a basic cationic dye, has been removed from

Table 3: Parameters Langmuir, Freundlich and Tempkin constants.

Absorbents	Langmuir parameters				Freundlich parameters			Tempkin parameters		
	b (L/mg)	Q_m (mg/g)	R^2	R_L	1/n	K_F (mg/g)	R^2	B (J/mol)	K_T (L/g)	R^2
CS	7.96	17.95	**0.9948**	0.111	0.28	16.31	0.9888	3.21	142.59	0.9887

Table 4: Comparison of adsorption capacity of candle soot with other literature value.

Precursors	Adsorption capacity Q_m (mg/g)	References
Candle soot	24.88	[4]
Candle soot	10.2	[26]
KOH-candle soot	24.4	[26]
Candle Soot	17.95	Present study

aqueous solution using prepared CS as an adsorbent. Langmuir isotherm and Temkin isotherm model revealed the chemisorption type of adsorption in candle soot.

Data Availability Statement

Supplementary data to this article can be found online at http://sciencemuseum.gov.np/.

Acknowledgement

Authors are thankful to Nepal Academy of Science and Technology (NAST) for XRD measurement. We are also grateful to Dr. Bipeen Dahal, Chonbuk National University, South Korea for SEM and EDS analysis.

References

[1] Singh, G. 2019. Applications in Energy Harvesting. In Summers Scholl (Eds.), *Fabrication and Application of Nanomaterials*. McGraw Hill, United States.

[2] Asim, N., Amin, M. H., Alghoul, M. A., Sulaiman, S. N. A., Razali, H., Akhtaruzzaman, M., Amin, N. & Sopian, K. 2021. Developing of chemically treated waste biomass adsorbent for dye removal. *Journal of Natural Fibers*. **18**(7): 968–977. Doi: https://doi.org/10.1080/15440478.2019.1675214

[3] Shen, Y. 2018. Rice Husk-derived activated carbons for adsorption of phenolic compounds in water. *Global Challenges*. **2**(12): 1800043. Doi: https://doi.org/10.1002/gch2.201800043

[4] Singh, G., Sharma, M. and Vaish, R. 2019. Tunable surface adsorption and wettability of candle soot coated on ferroelectric ceramics. *Journal of Advanced Research*. **16**: 35. Doi: https://doi.org/10.1016/j.jare.2018.12.005

[5] Pagels J., Wierzbicka A., Nilsson E., Isaxon C., A. Dahl., Gudmun--dsson A., Swietlicki E. and Bohgard M. 2009. Chemical composition and mass emission factors of candle smoke particles. *Journal of Aerosol Science.* **40**(3): 193–208.

[6] Sunderland P. B., Quintiere J. G., Tabaka G. A., Lian D. and Chiu C. W. 2011. Analysis and measurement of candle flame shapes. *Proceedings of the Combustion Institue.* **33**: 2489-2496.

[7] Kuszlik A. K., Meyer G., Heezen P. A. M. and Stepanski M. 2010. Morphological characterization of soot from the combustion of candle wax. *Journal of Chemical Engineering Research D.* **88**: 1279–1283.

[8] Zaky M. T. and Mohamed N. H. 2010. Comparative study on separation and characterization of high melting point macro-and micro-crystalline waxes. *Journal of Taiwan Institute of Chemical Engineering*. **41**:360–366.

[9] Zai S., Zhen H. and Jia-song W. 2006. Studies on the size distribution, number and mass emission factors of candle particles characterized by modes of burning. *Journal of Aerosol Science*. **37**:1484–1496.

[10] Tumolva, L., Park, J. Y., Kim, J. S., Miller, A. L., Chow, J. C. and Watson, J. G. 2010. Morphological and elemental classification of freshly emitted soot particles and atmospheric ultrafine particles using the TEM-EDS. *Aerosol Science and Technology*. **44**(3): 203-210.

[11] Joshi P., Lawaju U. and KC A. 2023. Lampblack of soybean oil as a low-cost electrode material in supercapacitor application. *Scientific World.* **16**(16): 94-99

[12] Yang Y., Fei Z. and Li Q. 2026.Candle-derived carbon soot nanoparticles as photothermal agents for controlled opening of the blood–brain barrier. *Results in Chemistry*. **23**: 103128

[13] Sahoo, B. N. & Kandasubramanian, B. 2014. An experimental design for the investigation of water repellent property of candle soot particles. *Materials Chemistry and Physics*. **148**(1):134–142. Doi: https://doi.org/10.1016/j.matchemphys.2014.07.022

[14] Mulay, M. R., Chauhan, A., Patel, S., Balakrishnan, V., Halder, A. & Vaish, R. 2019. Candle soot: journey from a pollutant to a functional material. *Carbon*. **144**: 684–712.

[15] Hadef R., Geigle K. P., Meier W. and Aigner M. 2010. Soot characterization with laser-induced incandescence applied to a

[16] laminar premixed ethylene-air flame. *International Journal of Thermal Science*. **49**: 1457–1467.

[17] Hussein T., Glytsos T., Ondracek J., Dohanyosova P., Zdimal V., Hameri K., Lazaridis M., Smolik J. and Kulmala M. 2006. Deposition rate on smooth surfaces and coagulation of aerosol particles inside a test chamber. *Journal of Atmospheric Environment*. **40**: 4285 – 4307.

[18] Takaki N. & Sekimoto H. 2008. Potential of candle reactor on sustainable development and strengthened proliferation resistance. *Progress in Nuclear Energy*. **50**(2): 114-118.

[19] Allouche, F. N. & Yassaa, N. 2018. Potential adsorption of methylene blue from aqueous solution using green macroalgae Posidonia oceanica. *IOP Conference Series: Materials Science and Engineering*. **323**(1): 012006.

[20] Nunes, C. A. & Guerreiro, M. C. 2011. Estimation of surface area and pore volume of activated carbons by methylene blue and iodine numbers. *Quimica Nova*. **34**(3): 472–476.
Doi: https://doi.org/10.1590/S0100-40422011000300020

[21] Ghalehkhondabi, V., Fazlali, A. & Ketabi, K. 2021. Synthesis and characterization of modified activated carbon (MgO/AC) for methylene blue adsorption: optimization, equilibrium isotherm and kinetic studies. *Water Science and Technology*. **83**(7):1548–1565. Doi: https://doi.org/10.2166/wst.2021.016.

[22] Kanakaraj, R. & Sudakar, C. 2020. Candle soot carbon nanoparticles as high-performance universal anode for M-ion (M= Li^+, Na^+ and K^+) batteries. *Journal of Power Sources*. **458**: 228064.

[23] Rashid, M. U., Tahir, Z., Kim, S., Jang, J. I. & Kim, Y. S. 2021. Selective deposition of candle soot on a cellulose membrane for efficient solar evaporation. *ACS Omega*. **6**(46): 31366–31374.
Doi: https://doi.org/10.1021/acsomega.1c05348.

[24] Ratih, D. & Siburian, R. 2018. The performance of graphite/n-graphene and graphene/n-graphene as electrode in primary cell batteries. *Rasayan Journal of Chemistry.* **11**(4): 1649-1656.

[25] Al-Ghouti, M. A. & Al-Absi, R. S. 2020. Mechanistic understanding of the adsorption and thermodynamic aspects of cationic methylene blue dye onto cellulosic olive stones biomass from wastewater. *Scientific Reports*. **10**(1): 15928.
Doi: https://doi.org/10.1038/s41598-020-72996-3.

[26] Fathihah M. A. and Khairunnisa1 M. P. 2021. Characteristics and carbon dioxide adsorption performance of candle soot-activated by potassium hydroxide. *IOP Conf. Series: Earth and Environmental Science.* **765**(1): 012087.
Doi: 10.1088/1755-1315/765/1/012087.